SUPPLEMENTAL MATERIAL

Kerr nonlinearity and plasmonic bistability in graphene nanoribbons

Thomas Christensen,[1,2] Wei Yan,[1,2] Antti-Pekka Jauho,[2,3] Martijn Wubs,[1,2] and N. Asger Mortensen[1,2]

[1] *Department of Photonics Engineering, Technical University of Denmark, DK-2800 Kgs. Lyngby, Denmark*
[2] *Center for Nanostructured Graphene, Technical University of Denmark, DK-2800 Kgs. Lyngby, Denmark*
[3] *Department of Micro- and Nanotechnology, Technical University of Denmark, DK-2800 Kgs. Lyngby, Denmark*

I. ITERATIVE PROCEDURE FOR NONLINEAR PROBLEM

We here discuss an iterative approach to solving the nonlinear equation

$$\lambda\phi(\mathbf{r}) = \lambda\phi_{\text{ext}}(\mathbf{r}) + \mathsf{V}\mathsf{D}[f[\phi]]\phi(\mathbf{r}), \tag{S1}$$

which is essentially just the driven correspondent of Eq. (4), and where we have emphasized the dependence of D on $\phi(\mathbf{r})$ through $f(\mathbf{r})$. The problem is evidently nonlinear, but can be solved efficiently by iteration with only linear algebra at each step. We follow the usual iteration scheme, as e.g. also used previously in the studies of bistability in dielectric waveguides [S1].

1. Compute a linear solution based on an initial guess of $f = f_{\text{ini}}$, i.e. solve Eq. (S1) with $\mathsf{D}[f[\phi]] \to \mathsf{D}[f = f_{\text{ini}}]$. Denote the obtained solution as $\phi^{[0]}$. Set the iteration step $m = 0$.
2. Calculate the mth guess at the occupation function $f^{[m]}$ from the potential $\phi^{[m]}$.
3. Compute the $(m+1)$th iteration by solving the linear system $\lambda\phi^{[m+1]} = \lambda\phi_{\text{ext}} + \mathsf{V}\mathsf{D}[f^{[m]}]\phi^{[m+1]}$.
4. Iterate steps 2 and 3 until convergence, otherwise update iteration step $m \to m+1$.

We impose convergence criteria corresponding to the simultaneous fulfillment of (with $\text{tol} = 10^{-5}$)

$$\max_{\mathbf{r}\in\Omega} \left|\phi^{[m+1]}(\mathbf{r}) - \phi^{[m]}(\mathbf{r})\right| \Big/ \max_{\mathbf{r}\in\Omega} \left|\phi^{[m]}(\mathbf{r})\right| < \text{tol}, \tag{S2a}$$

$$\max_{\mathbf{r}\in\Omega} \left|f^{[m+1]}(\mathbf{r}) - f^{[m]}(\mathbf{r})\right| \Big/ \max_{\mathbf{r}\in\Omega} \left|f^{[m]}(\mathbf{r})\right| < \text{tol}, \tag{S2b}$$

being of standard type for iterative approaches to nonlinearity [S1]. In all considered cases the iterative procedure converged after at most several hundred iterations. One exception should be mentioned however; the dipolar eigenmodes at field strengths 3×10^5 V/cm and 3.5×10^5 V/cm failed to converge after 1250 iterations for $k_\parallel \gtrsim 5$ and are consequently absent in Fig. 1 for these momenta. This could likely be remedied by a more elaborate stepping procedure, though such investigations have not been pursued further in this work.

Two additional extensions of the simple iterative scheme described above are employed. Firstly, for numerical stability we apply a linear mixing scheme for updating guesses on f, specifically we use $\mathsf{D}[f^{[m]}_{\text{mix}}]$ with $f^{[m]}_{\text{mix}} = (1-\xi_{\text{mix}})f^{[m-1]} + \xi_{\text{mix}}f^{[m]}$ in step 2 (mixing parameter $\xi_{\text{mix}} = 0.275$) rather than the unmixed $\mathsf{D}[f^{[m]}]$. Secondly, the initial guess f_{ini} is always taken from the previous field strength in ramping scenarios. This provides a significant numerical speed-up and, crucially, allows us to investigate hysteresis and bistability. The initial guess at the first field strength is naturally $f_{\text{ini}} = 1$.

For eigenmodal calculations where $\phi_{\text{ext}} = 0$, we normalize ϕ_n at each iteration to impose the desired ribbon-averaged field strength $\langle|\mathbf{E}(\mathbf{r})|\rangle$, and in addition determine ω_n from $\lambda_n(\omega_n)$ by numerically solving the equation in the complex frequency-plane.

A. Ramping details

As discussed in the main text, we compute, for each fixed energy $\hbar\omega$, solutions to Eq. (S1) for a ramp-array of many field-strengths, going both up and down. We here explicate the rather straightforward details

of this array: consider for each $\hbar\omega$ a ramp-array $\{E_{0,n}\}_{n=1}^{N}$ with $E_{0,n+1} > E_{0,n}$ and with $E_{0,1}$ sufficiently small to be considered a linear perturbation. Starting from $E_{0,1}$ we compute associated solutions and proceed, generally, to field strength $E_{0,n+1}$ with initial guesses on f and ϕ (provided to step 1 of the iterative procedure discussed in Section I) obtained from the nth solution. This defines the upward ramp, corresponding to slowly turning the incident intensity up. Upon reaching $n = N$ we invert the procedure and follow a downward ramp, in the pattern $E_{0,n} \to E_{0,n-1}$, corresponding to slowly turning the intensity down.

II. MATRIX REPRESENTATION OF V AND D IN A DISCRETIZED BASIS

We here elaborate the reduction of the differential and integral operators D and V to matrix representations $\mathbf{D}$ and $\mathbf{V}$ using an equidistant discrete basis. Specifically, we discuss the 1D ribbon case, although the generalization to general 2D restrictions is straightforward. Specifically, we imagine a system in the xy-plane, translationally invariant along y and with finite extent along x. For simplicity, we assume just a single ribbon, such that x is limited to the simple domain $x \in [0, 1]$. Furthermore, as the operators necessarily act on a potential $\phi(\mathbf{r})$, we impose translational invariance along y by the decomposition $\phi(\mathbf{r}) = \phi(x)e^{ik_\parallel y}$.

Starting with the differential operator D, we consider its operation onto $\phi(\mathbf{r})$, which takes the form $\mathsf{D}\phi(\mathbf{r}) = \partial_x[f(x)\partial_x\phi(x)]e^{ik_\parallel y} - k_\parallel^2 f(x)\phi(x)e^{ik_\parallel y}$. By extension, we define the operation of D onto the single-variable function $\phi(x)$ through $\mathsf{D}\phi(x) \equiv \partial_x[f(x)\partial_x\phi(x)] - k_\parallel^2 f(x)\phi(x)$. To proceed, we introduce a discretization of the x-coordinates as $\{x_j\}_{j=1}^{N}$ with associated values $\phi_j \equiv \phi(x_j)$ and $f_j \equiv f(x_j)$ (we take $N = 150$, being well-converged in all considered cases). Though not strictly necessary, we assume equidistant x_j with constant spacing $x_{j+1} - x_j = a$, see Fig. S1.

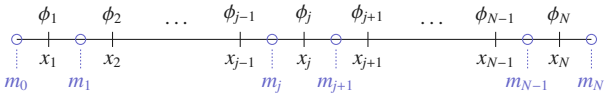

FIG. S1 Sketch of the discretization approach applied to a single ribbon.

The matrix elements D_{jl} of the finite-element representation of D is then defined by $\mathsf{D}\phi_j = \sum_l D_{jl}\phi_l$. The elements can be deduced using finite differences at the midpoints. Specifically, using central differences $\partial_x[f_j\partial_x\phi_j] \simeq a^{-1}(m_j - m_{j-1})$ where m_j defines midpoint-values of the function $m(x) \equiv f(x)\partial_x\phi(x)$ such that $m_j \simeq (2a)^{-1}(f_{j+1} + f_j)(\phi_{j+1} - \phi_j)$, see Fig. S1. For all interior points, $j \in [2, N-1]$, this then allows a decomposition of D_{jl} as the tridiagonal matrix

$$D_{jl} = \tfrac{1}{2a^2}\Big[\delta_{j-1,l}(f_{j-1} + f_j) - \delta_{jl}(f_{j-1} + 2f_j + f_{j+1}) + \delta_{j+1,l}(f_j + f_{j+1})\Big] - \delta_{jl}k_\parallel^2 f_j. \tag{S3a}$$

At the end-points $j = 1$ and $j = N$ we explicitly account for boundary conditions. Specifically, we ensure a vanishing of normal current, equivalent to the condition $\partial_x\phi(x) = 0$ for $x = 0$ and $x = 1$. In turn, this forces $m_0 = m_N = 0$, allowing

$$D_{1l} = \tfrac{1}{2a^2}(f_1 + f_2)(-\delta_{1,l} + \delta_{2,l}) - \delta_{1,l}k_\parallel^2 f_1, \tag{S3b}$$

$$D_{Nl} = \tfrac{1}{2a^2}(f_{N-1} + f_N)(\delta_{N-1,l} - \delta_{N,l}) - \delta_{N,l}k_\parallel^2 f_N. \tag{S3c}$$

As an alternative to taking explicit account of the boundary condition, one can allow a slightly larger x-range, and explicitly include points with $f(\mathbf{r}) = 0$ outside $\mathbf{r} \in \Omega$ – the step in $f(\mathbf{r})$ at $\mathbf{r} \in \partial\Omega$ then mimics an edge charge and accounts numerically for the boundary condition; such a procedure may be preferable in finite structures without any geometric symmetries compatible with a square grid.

The integral operator V is similarly amenable to explicit expression on the equidistant grid. Specifically, letting V operate on a function $g(\mathbf{r}) = g(x)e^{ik_\parallel y}$ one finds [S2; S3]

$$\mathsf{V}g(\mathbf{r}) = e^{ik_\parallel y}\int \mathrm{d}x'\, 2K_0(k_\parallel|x - x'|)g(x'), \tag{S4}$$

where $k_\parallel > 0$ is assumed and with K_0 denoting the zeroth order modified Bessel function of the second kind. Assuming a slowly varying $g(x)$ and an equidistant $\{x_j\}$ then allows a matrix decomposition of V via $\mathsf{V}g_j = \sum_l V_{jl} g_j$ where [S4]

$$V_{jl} = 2\int_{x_l-a/2}^{x_l+a/2} \mathrm{d}x'\, K_0(k_\parallel|x_j - x'|) = \pi \sum_{\tilde{x}=x_{jl}\pm a/2} \tilde{x}\Big\{K_0(k_\parallel|\tilde{x}|)\Big[\mathbf{L}_1(k_\parallel|\tilde{x}|) + \tfrac{2}{\pi}\Big] + K_1(k_\parallel|\tilde{x}|)\mathbf{L}_0(k_\parallel|\tilde{x}|)\Big\}, \tag{S5}$$

with $x_{jl} \equiv x_j - x_l$ and $\mathbf{L}_{0,1}$ denoting modified Struve functions of zeroth and first order.

A final detail which should be discussed is the special case $k_\parallel = 0$, where the kernel $K_0(k_\parallel|x - x'|)$ in Eq. (S5) diverges. Despite this divergence, finite and meaningful matrix elements can be retrieved by invoking charge conservation. Specifically, we note the small argument expansion $K_0(k_\parallel|x - x'|) \sim -\ln(|x - x'|) - \ln(k_\parallel) + \alpha$ where $\alpha = \ln(2) - \gamma_{\mathrm{EM}}$ (γ_{EM} is the Euler–Mascheroni constant) [S4]. The x'-independent term $-\ln(k_\parallel) + \alpha$ gives a contribution $[-\ln(k_\parallel) + \alpha]\int \mathrm{d}x'\, g(x')$ to Eq. (S4) and appears divergent as $k_\parallel \to 0$. Nevertheless, this contribution vanishes for the functions $g(\mathbf{r}')$ of relevance since they always represent induced charges [as evident from Eq. (3)] and obey charge conservation $\int \mathrm{d}x'\, g(x') = 0$. As such, the $k_\parallel = 0$ case can be calculated by simply letting $K_0(k_\parallel|x - x'|) \to -\ln(|x - x'|)$ in Eq. (S5) [S3], yielding $V_{jl} = -2\sum_{s=\pm} s(x_{jl} + s\frac{a}{2})\ln(|x_{jl} + s\frac{a}{2}|)$ for $k_\parallel = 0$.

This concludes the real-space discretization approach for reduction of the abstract operator equation of Eq. (4) into a matrix equation $\lambda\boldsymbol{\phi} = \mathsf{VD}\boldsymbol{\phi}$ with $\boldsymbol{\phi}$ denoting the vector form of ϕ_j.

III. PERTURBATION ESTIMATE OF THE NONLINEAR SHIFT OF EIGENFREQUENCIES

We here provide the derivations that allow the approximate result of Eq. (5). As we explain below, the approach relies on the formulation of a Hermitian eigenproblem followed by application of standard perturbation theory to a spatially inhomogeneous problem.

The compound operator VD defined in Eq. (4) is – though numerically practical – inconvenient for analytical considerations, because it is not symmetric. However, the problem can (of course) be cast as a Hermitian eigenproblem with eigenvalues λ_n [though, strictly speaking, only for real, positive occupation functions $f(\mathbf{r})$, which we restrict our analysis to here], as also noted recently in Refs. [S5; S6]. Specifically, consider the application of the scaled gradient operation $-\sqrt{f(\mathbf{r})}\nabla$ onto Eq. (3):

$$-\lambda\sqrt{f(\mathbf{r})}\nabla\phi(\mathbf{r}) = \sqrt{f(\mathbf{r})}\nabla\int_\Omega \mathrm{d}^2\mathbf{r}'\, V(\mathbf{r},\mathbf{r}')\nabla'\cdot\Big\{\sqrt{f(\mathbf{r}')}[-\sqrt{f(\mathbf{r}')}\nabla'\phi(\mathbf{r}')]\Big\}. \tag{S6}$$

Defining the scaled in-plane field $\boldsymbol{\xi}(\mathbf{r}) \equiv -\sqrt{f(\mathbf{r})}\nabla\phi(\mathbf{r})$ and manipulating further allows

$$\begin{aligned}
\lambda\boldsymbol{\xi}(\mathbf{r}) &= \sqrt{f(\mathbf{r})}\nabla\int_\Omega \mathrm{d}^2\mathbf{r}'\, V(\mathbf{r},\mathbf{r}')\nabla'\cdot[\sqrt{f(\mathbf{r}')}\boldsymbol{\xi}(\mathbf{r}')] \\
&\overset{a}{=} \sqrt{f(\mathbf{r})}\nabla\Big\{\int_\Omega \mathrm{d}^2\mathbf{r}'\,\nabla'\cdot\Big[V(\mathbf{r},\mathbf{r}')\sqrt{f(\mathbf{r}')}\boldsymbol{\xi}(\mathbf{r}')\Big] - \int_\Omega \mathrm{d}^2\mathbf{r}'\,[\nabla' V(\mathbf{r},\mathbf{r}')]\cdot[\sqrt{f(\mathbf{r}')}\boldsymbol{\xi}(\mathbf{r}')]\Big\} \\
&\overset{b}{=} -\sqrt{f(\mathbf{r})}\nabla\int_\Omega \mathrm{d}^2\mathbf{r}'\,\sqrt{f(\mathbf{r}')}[\nabla' V(\mathbf{r},\mathbf{r}')]\cdot\boldsymbol{\xi}(\mathbf{r}') \\
&\overset{c}{=} -\int_\Omega \mathrm{d}^2\mathbf{r}'\,\sqrt{f(\mathbf{r})f(\mathbf{r}')}[\nabla\otimes\nabla' V(\mathbf{r},\mathbf{r}')]\boldsymbol{\xi}(\mathbf{r}')
\end{aligned} \tag{S7}$$

with associated steps $a - c$ explicated below for convenience:

a. Application of chain rule to expand integrand.

b. The first integral term in step *a* vanishes, as can be deduced by application of the divergence theorem which transforms the term to $\oint_{\partial\Omega} V(\mathbf{r},\mathbf{r}')\sqrt{f(\mathbf{r}')}[\boldsymbol{\xi}(\mathbf{r}')\cdot\mathbf{n}']$. The integrand vanishes for all $\mathbf{r}' \in \partial\Omega$ due to the no-spill boundary condition on the induced current which forces $\boldsymbol{\xi}(\mathbf{r}')\cdot\mathbf{n}' = 0$ on $\mathbf{r}' \in \partial\Omega$.

c. The term $\sqrt{f(\mathbf{r})}\nabla$ is taken under the integral sign. ∇ operates on $\mathbf{r}$ and hence only on $V(\mathbf{r},\mathbf{r}')$. The operation $\nabla\{[\nabla' V(\mathbf{r},\mathbf{r}')]\cdot\boldsymbol{\nu}(\mathbf{r}')\}$ is rewritten in the equivalent outer-product form $[\nabla\otimes\nabla' V(\mathbf{r},\mathbf{r}')]\boldsymbol{\nu}(\mathbf{r}')$ with elements $[\nabla\otimes\nabla']_{ij} = \partial_{r_i}\partial_{r'_j}$.

We then define the operator M by its action on a field-ket $|\boldsymbol{\xi}\rangle$ [where, as usual, $\langle\mathbf{r}|\boldsymbol{\xi}\rangle \equiv \boldsymbol{\xi}(\mathbf{r})$]

$$\langle\mathbf{r}|\mathsf{M}|\boldsymbol{\xi}\rangle \equiv \int_\Omega \mathrm{d}^2\mathbf{r}'\ \sqrt{f(\mathbf{r})f(\mathbf{r}')}[\nabla\otimes\nabla' V(\mathbf{r},\mathbf{r}')]\boldsymbol{\xi}(\mathbf{r}'), \tag{S8}$$

with associated eigenspectrum $(-\lambda_n)$ and $|\boldsymbol{\xi}_n\rangle$:

$$(-\lambda_n)|\boldsymbol{\xi}_n\rangle = \mathsf{M}|\boldsymbol{\xi}_n\rangle. \tag{S9}$$

The operator M is evidently symmetric, positive semi-definite, and thus Hermitian. Aaccordingly, the eigenspectrum $\{-\lambda_n\}$ is non-negative and real; and the eigenkets $|\boldsymbol{\xi}_n\rangle$ are orthogonal $\langle\boldsymbol{\xi}_n|\boldsymbol{\xi}_{n'}\rangle = \delta_{nn'}\langle\boldsymbol{\xi}_n|\boldsymbol{\xi}_n\rangle$ and span the solution space for $\mathbf{r}\in\Omega$.

With these facts established, we can now discuss a perturbation treatment. Specifically, we consider the simple case where $f(\mathbf{r}) = f^{(0)} + \delta f^{(1)}(\mathbf{r})$ for $\mathbf{r}\in\Omega$ with "groundstate" $f^0 = 1$ and perturbation f^1 with strength δ. The corresponding expansion of $\mathsf{M} = \mathsf{M}^{(0)} + \delta\mathsf{M}^{(1)} + O(\delta^2)$ is found by expansion of Eq. (S8), yielding

$$\langle\mathbf{r}|\mathsf{M}^{(0)}|\boldsymbol{\xi}\rangle = \int_\Omega \mathrm{d}^2\mathbf{r}'\,[\nabla\otimes\nabla' V(\mathbf{r},\mathbf{r}')]\boldsymbol{\xi}(\mathbf{r}'), \tag{S10a}$$

$$\langle\mathbf{r}|\mathsf{M}^{(1)}|\boldsymbol{\xi}\rangle = \frac{1}{2}\int_\Omega \mathrm{d}^2\mathbf{r}'\,[f^{(1)}(\mathbf{r}) + f^{(1)}(\mathbf{r}')][\nabla\otimes\nabla' V(\mathbf{r},\mathbf{r}')]\boldsymbol{\xi}(\mathbf{r}'). \tag{S10b}$$

Since M is a Hermitian operator usual perturbation theory applies [S7]. Specifically, for a "groundstate" eigenspectrum $\{-\lambda_n^{(0)}, |\boldsymbol{\xi}_n^{(0)}\rangle\}$ the leading-order correction to the perturbed eigenvalue $\lambda_n = \lambda_n^{(0)} + \delta\lambda_n^{(1)} + O(\delta^2)$ is derivable by application of Eqs. (S10) [by using the $(\mathbf{r},\mathbf{r}')$-symmetry of the resulting equation]

$$\lambda_n^{(1)} = -\frac{\langle\boldsymbol{\xi}_n^{(0)}|\mathsf{M}_1|\boldsymbol{\xi}_n^{(0)}\rangle}{\langle\boldsymbol{\xi}_n^{(0)}|\boldsymbol{\xi}_n^{(0)}\rangle} = \lambda_n^{(0)}\frac{\langle\boldsymbol{\xi}_n^{(0)}|f^{(1)}|\boldsymbol{\xi}_n^{(0)}\rangle}{\langle\boldsymbol{\xi}_n^{(0)}|\boldsymbol{\xi}_n^{(0)}\rangle}.$$

For nonlinear purposes, we unfortunately do not know the exact perturbation $f^{(1)}$ as it should be determined self-consistently with the total field $|\boldsymbol{\xi}_n\rangle$. However, for low field-strengths this self-consistency can be neglected and we can approximate $f[|\boldsymbol{\xi}_n\rangle] \simeq f[|\boldsymbol{\xi}_n^{(0)}\rangle]$ with $|\boldsymbol{\xi}_n^{(0)}\rangle$ referring to the electric field predicted by a *linear* calculation (at the desired field strength). For the Kerr-type nonlinearity of Eq. (1) the resulting correction is therefore [assuming vanishingly small loss and noting $\boldsymbol{\xi}^{(0)}(\mathbf{r}) = \mathbf{E}^{(0)}(\mathbf{r})$ for $f^{(0)} = 1$]

$$\lambda_n^{(1)} \simeq -\lambda_n^{(0)}\frac{9}{8}\frac{\int_\Omega \mathrm{d}^2\mathbf{r}\,|\mathbf{E}^{(0)}(\mathbf{r})|^4}{E_{\mathrm{sat}}^2\int_\Omega \mathrm{d}^2\mathbf{r}\,|\mathbf{E}^{(0)}(\mathbf{r})|^2} = -\lambda_n^{(0)}\frac{9}{8}\frac{\langle|\mathbf{E}^{(0)}(\mathbf{r})|^4\rangle}{E_{\mathrm{sat}}^2\langle|\mathbf{E}^{(0)}(\mathbf{r})|^2\rangle}, \tag{S11}$$

with E_{sat} similarly evaluated at the linear resonance frequency $\omega_n^{(0)}$ associated with $\lambda_n^{(0)}$. Finally, the result of the main text, Eq. (5), is obtained by invoking the relation between eigenvalues λ_n and eigenfrequencies ω_n together with the lossless intraband conductivity $\sigma_{(1)}(\omega) \simeq \mathrm{i}e^2\epsilon_{\mathrm{F}}/\pi\hbar^2\omega$.

IV. QUALITATIVE ANHARMONIC OSCILLATOR MODEL

We review the basics of the simple anharmonic oscillator model [S8; S9], and discuss how it – in connection with a polarizability consideration – explains the π phase-shift observed for the bistable solutions in Fig. 3(c).

Before considering the nonlinear problem, we note first that the field profiles depicted in the red- and green-framed maps of Fig. 3(c), corresponding to energies just below and above the resonance energy $\hbar\omega^{(0)}$, exhibit the well-known π phase shift between each other. The phase-shift can be appreciated e.g. by inspection of the linear harmonic-oscillator polarizability $\alpha(\omega) \propto [(\omega^{(0)})^2 - \omega(\omega + i\gamma)]^{-1}$ which exhibits a sign-change of its real part as ω traverses the resonance at $\omega^{(0)}$: as a result, the induced dipole $p(\omega) = \alpha(\omega)E_0$ changes sign for $\omega \lessgtr \omega^{(0)}$, and correspondingly so for the induced fields. As noted in the main text, a similar phase-shift is observed in the bistable comparison, see black-framed modes in Fig. 3(c). Again, the origin of the sign change can be appreciated from a polarizability consideration by including a third-order anharmonic term to the harmonic oscillator model [S9]; we do this below.

In this qualitative model, we represent the induced dipole by a single (time-dependent) coordinate x, which obeys the simple equation of motion

$$m\ddot{\mathsf{x}} + m\gamma\dot{\mathsf{x}} = -efE_0(t) - \partial_{\mathsf{x}}U(\mathsf{x}), \tag{S12}$$

with an effective anharmonic restoring potential $U(\mathsf{x}) = \frac{1}{2}m(\omega^{(0)})^2\mathsf{x}^2 - \frac{1}{4}ma\mathsf{x}^4$, effective oscillator mass m, linear resonance $\omega^{(0)}$, anharmonic parameter a (note that $a > 0$ in our case cf. sign of Kerr conductivity), and coupling factor f. We seek the solution that oscillates at $\mathrm{e}^{-\mathrm{i}\omega t}$ in response to a perturbation $E_0(t) = E_0(\omega)\mathrm{e}^{-\mathrm{i}\omega t}$, i.e. the Kerr response; we denote this term by $\mathsf{x}^{(1\omega)}(\omega)\mathrm{e}^{-\mathrm{i}\omega t}$. Working with Eq. (S12) one finds (omitting declaration of ω-dependence)

$$m\Big[(\omega^{(0)})^2 - \omega(\omega + \mathrm{i}\gamma) - 3a|\mathsf{x}^{(1\omega)}|^2\Big]\mathsf{x}^{(1\omega)} = -efE_0. \tag{S13}$$

The polarizability $\alpha^{(1)}$ is linked to $\mathsf{x}^{(1\omega)}$ via the induced dipole $p^{(1\omega)} = -e\mathsf{x}^{(1\omega)} = \alpha^{(1\omega)}E_0$, allowing (ignoring loss, being nonessential for the present considerations)

$$\Big[(\omega^{(0)})^2 - \omega^2 - 3ae^{-2}|\alpha^{(1\omega)}|^2E_0^2\Big]\alpha^{(1\omega)} = e^2f/m. \tag{S14}$$

For the bistable scenarios the term $(\omega^{(0)})^2 - \omega^2$ is always positive, see e.g. Figs. 2 and 3. Depending on the magnitude of $3ae^{-2}\alpha^{(1\omega)}E_0^2$ relative to $(\omega^{(0)})^2 - \omega^2$ it is then clear that polarizability-solutions of opposing sign can arise, depending on the sign of the terms bracketed on the left-hand side of Eq. (S14). Furthermore, if we denote the positive and negative solutions $\alpha_+^{(1\omega)}$ and $\alpha_-^{(1\omega)}$, respectively, it can then be deduced by direct inspection of Eq. (S14) that $|\alpha_+^{(1\omega)}| < |\alpha_-^{(1\omega)}|$. In other words, the induced dipole – and hence the induced fields – of the positive solution should be lower than its negative counterpart; upon identifying the lower branches of Fig. 3(b) with $\alpha_+^{(1)}$ and vice versa for the upper branch, we see that this is exactly the case. As such, the anharmonic model describes not only the phase-shift, but also the magnitude interrelationship. Lastly, we mention for completeness that the anharmonic model describes also a third solution, which, however, is physically irrelevant as it is unstable (and correspondingly is not found in the iterative procedure employed in this study, nor in experimental investigation).

V. PLASMONIC SOLITONS AND THE NONLINEAR SCHRÖDINGER EQUATION

As a simple, practical example of our general considerations, we here discuss how our results can be applied to study 1D plasmonic solitons within the framework of the 1D nonlinear Schrödinger equation (NLSE). Specifically, pulse propagation along the ribbon's y-direction (i.e. along $k_\parallel$) can be well-described by the NLSE under the same assumptions underlying its use in nonlinear fiber optics [S10]. For a slowly varying pulse (in y) with center frequency ω_0 and associated center momentum $k_\parallel^0$, and under the assumption of negligible propagation loss the NLSE reads [S8; S10]

$$\mathrm{i}\frac{\partial\tilde{A}(y,\tau)}{\partial y} - \frac{\beta_2}{2}\frac{\partial^2\tilde{A}(y,\tau)}{\partial\tau^2} + \gamma_{\mathrm{nl}}|\tilde{A}(y,\tau)|^2\tilde{A}(y,\tau) = 0, \tag{S15}$$

expressed in the retarded time-frame $\tau = t - \frac{\partial k_\parallel}{\partial\omega}\big|_0 y$ with $\big|_0$ indicating evaluation in the low-field limit at center frequency and momentum ω_0 and $k_\parallel^0$ with all complementary parameters held fixed. Here $\tilde{A}(y,\tau) = A(y,t)$ is the y-dependent envelope function of the field amplitude $E(y,t) = A(y)\mathrm{e}^{\mathrm{i}k_\parallel^0 y - i\omega_0 t}$. In the 1D treatment, $E(y,t)$ corresponds physically to the y-dependence of the x-averaged amplitude. Finally, parameters β_2 and γ_{nl} give the group velocity dispersion $\beta_2 \equiv \frac{\partial^2 k_\parallel}{\partial\omega^2}\big|_0$ and the nonlinear parameter $\gamma_{\mathrm{nl}} \equiv \frac{\partial k_\parallel}{\partial|\tilde{A}|^2}\big|_0$.

Our main point here is to highlight that the coefficients β_2 and γ_{nl} can be analytically expressed for moderate field strengths in terms of eigenvalues $\lambda_n(k_\parallel)$, inhomogeneity parameter κ, saturation field E_{sat}, and ribbon setup ϵ_{F} and W. In particular, working in the intraband approximation where $\hbar\omega(k_\parallel) = \hbar\Omega\sqrt{-\lambda(k_\parallel)}$, with $\hbar\Omega \equiv (2\pi)^{-1}\sqrt{e^2\epsilon_{\mathrm{F}}/\varepsilon_0 W}$, allows obtention of

$$\beta_2 = -\frac{4}{\Omega^2}\left(\frac{\partial\lambda(k_\parallel)}{\partial k_\parallel}\Big|_0\right)^{-1}\left[\frac{1}{2} - \lambda(k_\parallel^0)\frac{\partial^2\lambda(k_\parallel)}{\partial k_\parallel^2}\Big|_0\left(\frac{\partial\lambda(k_\parallel)}{\partial k_\parallel}\Big|_0\right)^{-2}\right]. \tag{S16}$$

Similarly, using $\mathrm{d}\omega = \frac{\partial\omega}{\partial k_\parallel}\big|_0 \mathrm{d}k_\parallel + \frac{\partial\omega}{\partial|\tilde{A}|^2}\big|_0 \mathrm{d}|\tilde{A}|^2 = 0$ and Eq. (5), allows expression of γ_{nl}

$$\gamma_{\mathrm{nl}} = \frac{\partial k_\parallel}{\partial|\tilde{A}|^2}\bigg|_0 = -\frac{\partial\omega}{\partial|\tilde{A}|^2}\bigg|_0 \left(\frac{\partial\omega}{\partial k_\parallel}\bigg|_0\right)^{-1} \qquad \text{where } \frac{\partial\omega}{\partial|\tilde{A}|^2}\bigg|_0 = \frac{-9}{16}\frac{\kappa\omega_0}{E_{\mathrm{sat}}^2} \text{ and } \frac{\partial\omega}{\partial k_\parallel}\bigg|_0 = \frac{-\Omega}{2[-\lambda(k_\parallel^0)]^{1/2}}\frac{\partial\lambda(k_\parallel)}{\partial k_\parallel}\bigg|_0,$$
$$= \frac{9}{8}\frac{\kappa}{E_{\mathrm{sat}}^2}\lambda(k_\parallel^0)\left(\frac{\partial\lambda(k_\parallel)}{\partial k_\parallel}\bigg|_0\right)^{-1}, \tag{S17}$$

where we have used that $\langle|\mathbf{E}^{(0)}|^2|\rangle \simeq |\tilde{A}|^2$ to linear order, and where κ denotes the inhomogeneity parameter defined by $\langle|\mathbf{E}^{(0)}|^4\rangle \equiv \kappa\langle|\mathbf{E}^{(0)}|^2\rangle^2$. Note that κ is also (weakly) momentum-dependent and hence evaluated at $k_\parallel^0$; higher-order corrections $\propto \frac{\partial\kappa}{\partial k_\parallel}\big|_0$ are neglected.

Crucially, for negative β_2 Eq. (S15) exhibits an analytical (bright) soliton solution, with spatial phase factor $\delta k_\parallel \equiv -\beta_2/2\tau_0^2$ [S8]

$$\tilde{A}(y,\tau) = \tilde{A}^0 \mathrm{sech}(\tau/\tau_0)\mathrm{e}^{\mathrm{i}\delta k_\parallel y}, \tag{S18}$$

provided the pulse width τ_0 and maximum amplitude $\tilde{A}^0$ are interrelated by

$$N^2 \equiv \frac{\gamma_{\mathrm{nl}}|\tilde{A}^0|^2\tau_0^2}{|\beta_2|} = 1. \tag{S19}$$

In Fig. S2 we plot $\beta_2\Omega^2$ and $\gamma_{\mathrm{nl}}E_{\mathrm{sat}}^2$ – which are dimensionless, universal functions of the ribbon, independent of setup parameters ϵ_{F} and W – as functions of $k_\parallel^0$ for the first few eigenmodes of the nanoribbon ($n = 0, 1, \ldots$, corresponding to monopole, dipole, etc.). Apart from the monopole and dipole, the modes exhibit simultaneously positive γ_{nl} and negative β_2 in the entire or most of the considered $k_\parallel^0$-region [restricted to small $k_\parallel^0$ to ensure validity of Eq. (S15)]. Accordingly, fundamental soliton solutions, of the type in Eq. (S18), are allowed for these modes for appropriate values of $|\tilde{A}^0|^2\tau_0^2$. The dipole mode exhibits a small region of feasible soliton parameters for larger $k_\parallel^0 \gtrsim 0.49$.

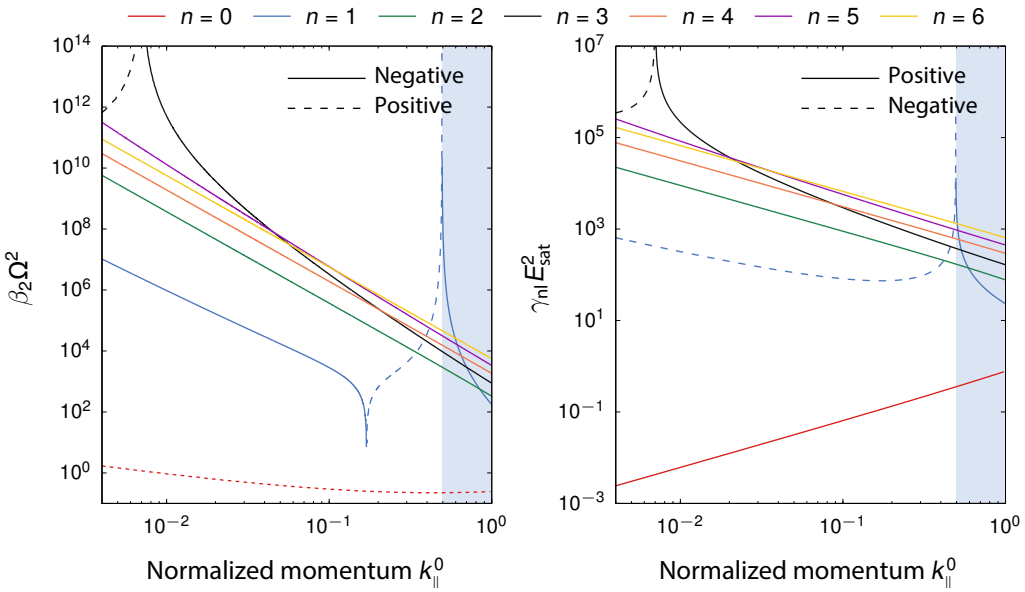

FIG. S2 Universal parameters $\beta_2\Omega^2$ and $\gamma_{\mathrm{nl}}E_{\mathrm{sat}}^2$ for the nth eigenmodes of the nanoribbon. Sign is indicated by line style. Momentum regions where full lines coexist, i.e. where $\beta_2 < 0$ and $\gamma_{\mathrm{nl}} > 0$, indicate feasible soliton regimes. This region is highlighted for the dipole in gray shading.

References

[S1] X.-H. Wang, *Finite Element Methods for Nonlinear Optical Waveguides*, Advances in Nonlinear Optics, Vol. 2 (Gordan and Breach Publishers, 1995).

[S2] I. Gradshteyn and I. Ryzhik, *Table of Integrals, Series, and Products*, 7th ed. (Elsevier Academic Press, 2007).

[S3] W. Wang and J.M. Kinaret, Phys. Rev. B **87**, 195424 (2013).

[S4] National Institute of Standards and Technology, "Digital library of mathematical functions," Release 1.0.9 of 2014-08-29.

[S5] K.A. Velizhanin, Phys. Rev. B **91**, 125429 (2015).

[S6] F.J. García de Abajo and A. Manjavacas, Faraday Discuss. **178**, 87 (2015).

[S7] S. Gasiorowicz, *Quantum physics*, 3rd ed. (John Wiley & Sons, 2003).

[S8] R.W. Boyd, *Nonlinear Optics*, 3rd ed. (Academic Press, 2008).

[S9] J.D. Cox and F.J. García de Abajo, Nat. Commun. **5**, 5725 (2014).

[S10] G.P. Agrawal, J. Opt. Soc. Am. B **28**, A1 (2011).